



# Dispersion modeling of gaseous and particulate matter emissions from aircraft activity at Chania Airport, Greece

Minas Makridis<sup>1</sup> · Mihalis Lazaridis<sup>1</sup>

Received: 2 April 2019 / Accepted: 20 May 2019  
© Springer Nature B.V. 2019

## Abstract

Aircraft emissions from Landing and Take-Off (LTO) cycles at Chania airport (Crete), Greece were estimated for the year 2016 adopting the *International Civil Aviation Organization* (ICAO) methodology and using daily data from air traffic. The AERMOD Gaussian dispersion model was elaborated to determine the ground-level concentrations of air pollutants emitted from the aircraft engines. Emissions of CO, NO<sub>x</sub> as NO<sub>2</sub>, SO<sub>2</sub>, CO<sub>2</sub>, PM<sub>2.5</sub> mass, and particle number from aircraft engines were evaluated and ground-level concentrations of these pollutants were determined. The aircraft emissions were mainly derived from the ground-level parts of the LTO cycle. The AERMOD model referring to the 1-h average concentrations has revealed that there were 20 exceedances of NO<sub>2</sub> concentrations above the value of 200 µg/m<sup>3</sup>; two more than the regulated threshold described in the European Union Directive 2008/50/EC. The exceedances were calculated mostly during the summer period which coincides with the touristic period. High number concentrations of particles were also simulated close to the airport with yearly average values close to 10,000 particles per cm<sup>3</sup> at the airport area. Contrary, the contribution from aircraft LTO cycles to the ground-level concentration of CO, SO<sub>2</sub>, and PM<sub>2.5</sub> mass was below the air quality threshold values.

**Keywords** Aircraft · Emissions · LTO · Dispersion · AERMOD

## Introduction

Gaseous and particulate matter emissions associated with aircraft activity are of major concern since air pollutants deteriorate the local air quality and may contribute to the greenhouse effect and the global climate change (Campbell et al. 2018). The air pollutants from aircraft engine exhausts include NO<sub>x</sub>, SO<sub>x</sub>, CO, unburnt hydrocarbons (HCs), and particulate matter among others (Masiol and Harrison 2014). Engine exhausts also release CO<sub>2</sub> and H<sub>2</sub>O as they are the main products of the ideal combustion posing an environmental concern, too. In fact, aviation has been responsible for the 2% of the anthropogenic emissions of CO<sub>2</sub> in 1992 (IPCC 1999). In addition, particulate matter from exhausts of modern aircrafts has an

aerodynamic diameter of 0.1 µm or less (Petzold et al. 2003; Zhu et al. 2011; EMEP 2017). European air quality limits exist for fine particles (PM<sub>2.5</sub>) according to the Directive 2008/50/EC. Moreover, at high altitudes, the released H<sub>2</sub>O, contained in the exhaust gases leads to the formation of contrails and, consequently, to the formation of cirrus clouds. Eventually, cirrus clouds favor the local temperature increase as they absorb the electromagnetic radiation. There is also an impact of contrails on flight safety since they can influence the aircraft trajectories (Yin et al. 2018).

Elevated concentrations of NO<sub>x</sub> and air quality exceedances were measured in several international airports (Carslaw et al. 2006; Yang et al. 2018; Mazaheri et al. 2009; Yilmaz 2017). High concentrations of ultrafine particles were measured during takeoff activities at the Los Angeles International Airport (LAX) by Zhu et al. (2011), as well as, elevated concentrations of PM<sub>2.5</sub>, formaldehyde, and acrolein in the vicinity of the airport. Shirmohammadi et al. (2017) studied also the impact of the LAX to its vicinity and concluded that it is a major source of fine particles, PM<sub>2.5</sub> mass, and black carbon (BC). Furthermore, an increase of hydrocarbons and CO was measured in the vicinity of Marco Polo airport in Venice related to aircraft activities (Pecorari et al. 2016). The

**Electronic supplementary material** The online version of this article (<https://doi.org/10.1007/s11869-019-00710-y>) contains supplementary material, which is available to authorized users.

✉ Mihalis Lazaridis  
lazaridi@mred.tuc.gr

<sup>1</sup> Technical University of Crete, School of Environmental Engineering, Polytechnioupolis, 73100 Chania, Greece

meteorological conditions were found to be an important parameter for the dispersion of air pollutants emitted from aircraft activities using a Lagrangian model.

A numerical study focused on a large commercial airport of Turkey (Atatürk International Airport) was conducted using USEPA's AERMOD model (Kuzu 2018). The study examined the dispersion of NO<sub>x</sub>, CO, and unburnt hydrocarbons emitted from aircraft activities over a period of 1 year. The study concluded that aircraft emissions resulted to the exceedance of the annual NO<sub>x</sub> levels in the area under study. In addition, Simonetti et al. (2015) studied dispersion of gaseous emissions produced by aircraft activity using the AERMOD model and found also an exceedance of the air quality levels for NO<sub>x</sub> emissions.

In the present study, the environmental impact of aircraft activity in the local air quality from the Chania airport, Crete, Greece was examined which is one of the three commercial airports at the island of Crete. The AERMOD model used in the analysis in conjunction with an emission inventory for Landing and Take-Off (LTO) cycle of aircrafts at the Chania airport.

## Materials and methods

### Study of interest—Chania airport “Ioannis Daskalogiannis”

Chania airport “Ioannis Daskalogiannis” (ICAO code LGSA) is located at Akrotiri peninsula 11.2 km North East of the city of Chania at the western part of Crete, Greece. According to the Hellenic Civil Aviation Authority (HCAA), the geographical coordinates of the airport are 35°31'53" North, 24°09'04" East [Universal Transverse Mercator (UTM) coordinates of the airport are 3935709 Northing and 241691 Easting, expressed in meters], and the elevation is 149.4 m. These coordinates refer to the center of the main runway, which has been considered the center point of the modeled area in this study.

Moreover, according to the HCAA, the orientation of the main runway is 110°–290°, defining two respective alternative runway options for take-off and landing, i.e., “11” and “29,” depending on the prevailing wind direction. The main runway has a nominal length of 3348 m and a nominal width of 45 m. In parallel of the main runway, there are two taxiways, one in the northeast and one in the southwest direction. Both taxiways have the same length as the main runway. Only the northeast taxiway is used by civil aviation aircrafts. The present study refers exclusively to designated civil aviation aircraft movements recorded during the year 2016. Private aircraft movements have not been included in this study.

The commercial aircraft activity of the airport has been studied according to the fundamental concept of the Landing

and Take-Off (LTO) cycle which includes five discrete aircraft phases; approach below 3000 ft. and landing, arrival (taxi-in) to the parking area, departure (taxi-out) from the parking area, take-off, and climb out up to 3000 ft. (ICAO 2008).

Apart from taxi-in, taxi-out, and take-off phases, in which they are regarded as ground-level operations within the airport site, the rest ones cover a horizontal distance until the aircraft reduces its altitude from 3000 ft. to ground-level or reaches the altitude of 3000 ft. after take-off. The airport is equipped with instrumental landing system, and the approach route is consistent for all aircrafts. Additionally, the respective horizontal distance of the height of 3000 ft. has been determined by monitoring multiple B738 aircraft arrivals at the airport and departures, through a specialized web site (Flightradar 24 2018). The selection of this aircraft type has been made due to its common occurrence in several Greek airports.

The borders of the area under study have been established by taking into account the potential area of interest to be influenced from aircraft activities in the airport of Chania. Moreover, the vicinity of the airport to several nearby settlements could provide a good overview of the environmental impact of the produced emissions. These facts suggested that the optimal expansion of the studied area should be 24 km length by 16 km width, which equals to 384 km<sup>2</sup>.

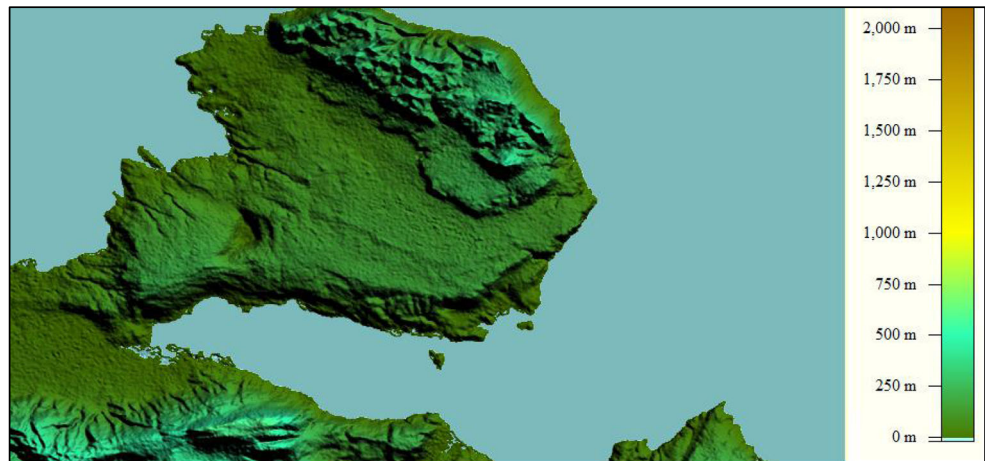
### AERMOD model

The present study has been conducted using the AERMOD Gaussian dispersion model (USEPA 2016). A variety of additional data were also incorporated in the model application. These include meteorological, geographical, land use, and emission data. The AERMOD model incorporates several preprocessors, the main processor of AERMOD, and the postprocessor of AERPLOT. The AERPLOT postprocessor has not been used in this study since the output data from AERMOD were visualized via a dedicated code in Matlab R2014b.

The AERMAP preprocessor requires a suitable digital elevation model (DEM) file which has been obtained from the United States Geological Survey (USGS 2018) site after the insertion of the coordinates of the four corners of the studied area. The DEM file type has been selected from the available menu as a Shuttle Radar Topography Mission (SRTM) 1 Arc-Second Global. The acquired file was a geotiff image much bigger than the requested one. The coordinates of the requested file were [35°, 36°] north and [24°, 25°] east, covering a large portion of the west and the central parts of the island of Crete.

The acquired DEM file had to be inserted to Global Mapper software for further visualization. After the insertion, the file has been cropped to the desired coordinates. Global Mapper revealed all the details about the studied area topography (see Fig. 1). The airport is located on a plane site of

**Fig. 1** Studied area geographical characteristics (viewed with Global Mapper)



average elevation of 150 m on Akrotiri peninsula. On the north of the airport, there is a 10-km mountain range with a maximum elevation of 527 m. The foothills of this formation create a plain with an elevation of 200 m. There is also another mountainous formation at the south part of the studied area, with a maximum elevation of 609 m. The land-use type of the land area is basically rural. Souda Bay is a natural port located in the middle of the area which forms a basin between these geological entities. The west coast of Akrotiri borders with Chania Gulf, whereas the northeast coast borders with Cretan Sea. The topography of the area is considered of great importance during the study of the emissions dispersion models.

The delineation of the land portion of the studied area has been carried out in MatLab environment (R2014b). Therefore, a dedicated code has been developed to produce the shoreline. The output file from AERMAP preprocessor which included the coordinates of the receptors has been used for this purpose. Since the receptors have been distributed in AERGRID preprocessor with a spacing of 200 m, the precision of the created shoreline in the map has a resolution of 200 m. The constructed map has been used as a background map so the results of the dispersion modeling could be super positioned. Both latitude and longitude coordinates have been expressed in UTM [m]. The map incorporates a grid which defines 24 square blocks of 16 km<sup>2</sup>, since both latitude and longitude axes have been divided into 4-km intervals. Moreover, the intersection of the middle distances of the two axes coincides with the center of the main runway. Finally, the airport main runway is depicted as a black color line in the map. The constructed map is shown in [Supplement](#).

### Meteorological data

The weather station of Chania airport is coded as 16746 according to World Meteorological Organization (WMO). The required meteorological data for the conduction of this study

included wind data, i.e., direction [degrees] and speed [m/s], barometric pressure [mb], dry bulb temperature [°C], relative humidity [%], precipitation [mm/h], and total cloud cover [tenths]. Wind data have been provided from a meteorological site (Ogimet 2017), whereas the rest of the data have been provided from the Hellenic National Meteorological Service (HNMS).

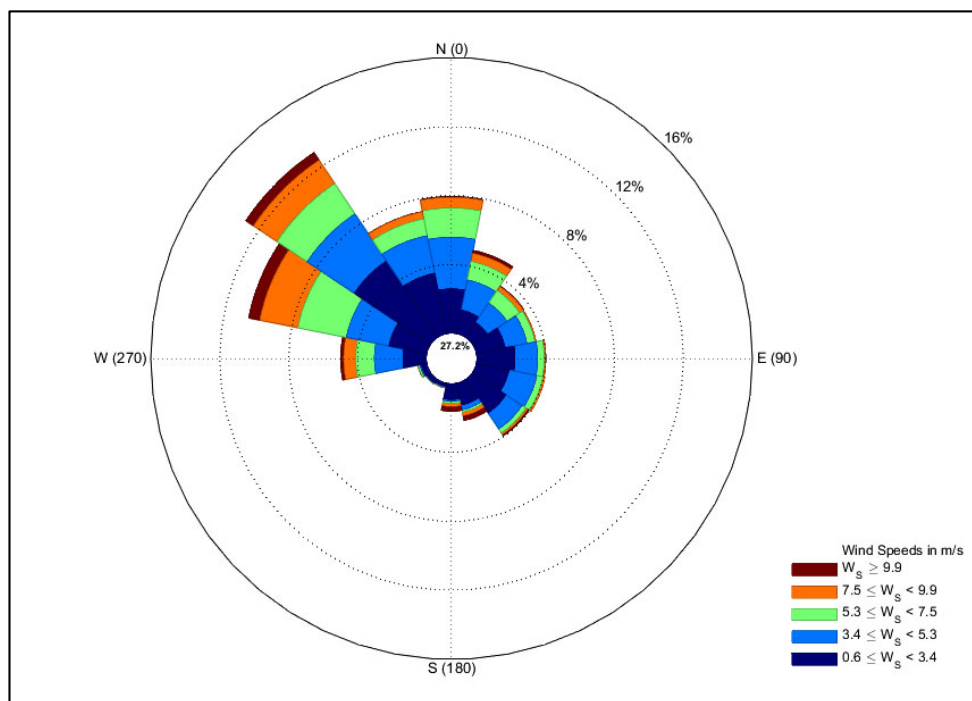
Hourly measurements of wind data for the year 2016 are shown in the wind rose diagram of Fig. 2. In respect to wind direction, it can be noticed that there has been a prevalence of north west direction by a percentage of 13%. The second dominant direction was west-northwest by 10.5%, while the third one was north by 8%. The predominance of the first two recorded wind directions justified an exclusive westward runway use option, in this study.

Wind speed has been separated into five intervals. The first interval, i.e., [0.6, 3.4) m/s, occurred during the 29% of the speed measurements and the second one, i.e., [3.4, 5.3) m/s, occurred at 22% of the measurements. Only 2.4% of the speed values were sorted above 9.9 m/s, whereas calms occupied the 27% of the measurements.

### Emission sources

All of the source types have been defined as area sources. Five rectangular emission sources have been defined in order that a typical LTO cycle could be modeled. The initial coordinates and the respective dimensions of take-off, taxi-in, and taxi-out sources have been provided by HCAA. The initial coordinates of the climb-out source have been determined by expanding the initial coordinates of the take-off source to the westward direction, up to the point that the horizontal distance refers to the altitude of 3000 ft. The initial coordinates of the approach/landing source has been set at the lowest right corner of the take-off source rectangular. All the initial coordinates of the sources have been inserted to the AERMAP preprocessor, and they have been further processed in AERMOD processor,

**Fig. 2** Windrose profile of Chania airport during the year 2016



where their respective dimensions and the angle of rotation have been also declared.

According to the wind profile of the airport, which showed that there has been a predominance of mainly north west and secondarily west-northwest winds, the emission sources have been set-up under the assumption that the majority of the aircraft movements had been carried out using the “29” runway option. Starting from the parking area, the aircrafts have been taxiing-out moving southeast via the northeast taxiway, taking-off using the 29 runway and climbing out up to 3000 ft. Similarly, after descending from 3000 ft., they have been approaching and landing moving northwest, and taxiing-in the parking area. This scenario is provided in the Supplement along with the defined emission sources.

The emission sources which refer to take-off, taxi-in, and taxi-out have been regarded as ground-level sources; thus, their pollutants’ release height has been set to 2 m above the ground, which is technically an average height of the aircraft engine exhausts. The definition of climb out and approach/landing as area sources was in contrast with the fact that the release height is not steady during these phases due to the respective aircraft constant loss or gain of flight altitude. Therefore, the release height for these emission sources has been placed at the altitude level of 1500 ft., which is the average altitude between 3000 ft. and the ground. However, the emissions produced from climb out and approach/landing had a small contribution to the total emissions as it will be discussed in the “Results” section. Numerous test runs have been conducted by lowering the release height below 1500 ft. up to 300 ft., with small differentiations on the results. This

could be explained by the fact that the emissions at these heights disperse in a very large volume, and their contribution to the total emissions is moderate. The current study examined exclusively the emissions originating from LTO cycles, since the emissions from aircrafts’ auxiliary power units (APUs) have not been studied. In addition, emissions from support and passenger vehicles inside and near the airport have not been studied either. However, elevated exposure levels for airport personnel during idling activities were calculated for formaldehyde and acrolein according to Testa et al. (2013). Finally, wear and tear particles emitted from aircrafts were not considered in the current simulations.

### Traffic composition-aircraft engine emissions

Throughout the year 2016, Chania airport serviced 135 different types of aircrafts which performed 10,324 LTO cycles. However, the frequency of occurrence was not the same for all these aircrafts. The composition of the air traffic has been determined with traffic data provided by the HCAA.

Although the number of aircraft types was quite large (135), the majority of LTO cycles have been performed by only 6 aircraft types that occupied 87% of the traffic composition. The remaining 13% refers to the group of aircrafts with a relatively small presence (below 180 LTOs) in the whole traffic load. Boeing aircrafts occupied over 50% of the traffic, since 737–800 had the biggest share of the flight activity (49%). On the other hand, Airbus aircrafts had the second largest traffic portion with a total of 33%.

Engine emission calculations have been carried out by matching every aircraft type with the respective engine model according to ICAO (2011). The number of engines which is also an input parameter for the emission calculations was found in EMEP (2017). Emission factors from carbon monoxide (CO) and nitrogen oxides (NO<sub>x</sub>) were taken from the ICAO (2011) database.

Emissions have been calculated according to the simple approach (option B) (ICAO 2011). This approach includes the total activity of all different aircraft types operated in the studied airport, which can be expressed as

$$E_i = \sum_{j=1}^m A_j \times \sum_{k=1}^p TIM_{jk} \times FF_{jk} \times E_{ijk} \times Ne_j \quad (1)$$

where,  $E_i$ : total emissions of pollutant  $i$  produced by all aircraft types [g];  $j$ : aircraft type;  $m$ : total number of aircraft types operated in the airport;  $k$ : LTO mode (approach/landing, taxi-in, taxi-out, take-off, climb out);  $p$ : total number of LTO modes (i.e. five);  $A_j$ : total activity of aircraft type  $j$  [LTOs];  $TIM_{jk}$ : time-in-mode for mode  $k$  for aircraft type  $j$  [s];  $FF_{jk}$ : fuel flow for mode  $k$  for each engine used on aircraft type  $j$  [kg/s];  $E_{ijk}$ : emission index for pollutant  $i$  in mode  $k$  for engine used on aircraft type  $j$  [g/kg of fuel];  $Ne_j$ : number of engines used on aircraft type  $j$ .

The emission rates have been calculated by considering the emissions produced from each source during the respective sum of LTO's modes. These emissions have been divided by both the studied period and the emission source area where the LTO modes have taken place. Consequently, the emission rates are given by the following equation:

$$Er_i = \frac{\sum_{j=1}^m A_j \times TIM_{jk} \times FF_{jk} \times E_{ijk} \times Ne_j}{Et \times Es} \quad (2)$$

where  $Er_i$ : emission rate of pollutant  $i$  produced by all aircraft types during LTO mode  $k$  [g/(s·m<sup>2</sup>)],  $Et$ : total time of studied period [s], and  $Es$ : emission source area [m<sup>2</sup>].

Furthermore, the emission factor indices for particles per unit of consumed fuel were obtained from the study of Kinsey et al. (2010). This study has introduced a relationship between engine fuel consumption [kg/h] and the number of particles per kg of fuel burnt ( $EI_n$ ) which is given by the following equation:

$$EI_n = m \ln(\text{fuel flow}) + b \quad (3)$$

where the values for the constants  $m$  and  $b$  were set equal to  $(-2)$  and  $(2 \times 10^{17})$  respectively concerning the CFM56 engines. The Pratt and Whitney engine PW40600 engines were considered of the same technological characteristics as PW4158, so the coefficient  $m$  of Eq. (3) has been set to  $(-2)$  and the term  $b$  has been set to  $(2 \times 10^{16})$ . In both cases, the selection of

the coefficient  $m$  and the term  $b$  has been made according to the experimentally determined values (Kinsey et al. 2010). Simulations were performed for the calculation of the average number concentration of particles at surface level for annual and 24-h basis. In the input file for the AERMOD, the particles were introduced in the PM<sub>0.1</sub> class, since emissions from modern aircraft exhausts contain exclusively ultrafine particles (Zhu et al. 2011; Petzold et al. 2003).

Airport traffic data for the year 2016 have been provided by the State Aviation Authority at Chania airport. Apart from taxi-in and taxi-out times which have been provided through personal communication with the mentioned authority, standard ICAO modal times have been used for the rest of the LTO phases, i.e., approach and landing, take-off and climb out. The duration of a typical LTO cycle at Chania airport is 1649 s (27.48 min). The entire set of modal times is given in Supplement.

The required engines data, i.e., fuel consumption and emission indices, have been selected from ICAO Engine Emissions Data Bank (ICAO 2018), which also provided information about the respective equipped power engine. Emission indices for CO and NO<sub>x</sub> have been taken directly from ICAO Engine Emissions Data Bank. Emission indices for CO<sub>2</sub> have been calculated by taking into account that 3.16 kg of CO<sub>2</sub> are emitted for every kg of consumed jet fuel (IPCC 2006). Emission indices for SO<sub>2</sub> have been determined considering that S content in fuel is 0.05% (IPCC 2006; ICAO 2011). The First Order Approximation (FOA version 3) methodology (ICAO 2011) has been used for the determination of particulate matter emissions. Several engine technical characteristics such as smoke number (SN), bypass ratio (BPR), and air to fuel ratio (AFR) were used for the calculations. SN and BPR have been selected from ICAO (2018), whereas default LTO values for AFR have been provided from ICAO (2011).

## Results and discussion

### LTO cycles emissions

The total number of LTO cycles performed by civil aviation aircrafts during the year 2016 at the Chania airport was 10,324. The total annual fuel consumption inside the examined area reached 9136 t, which resulted that 885 kg of fuel was consumed per LTO. The produced pollutants emissions were estimated according to the prescribed methodology of ICAO (2011). The total amount of emitted CO was estimated to be 66.4 t and the emitted amount of NO<sub>x</sub> has been estimated to be 137 t. Smaller amounts were estimated for PM<sub>2.5</sub> and SO<sub>2</sub> which were calculated to be 3 t and 9.2 t, respectively. Concerning the annual emissions of CO<sub>2</sub>, which have a direct effect on climate; annual CO<sub>2</sub> emissions reached 28,870 t.

The emissions per every separate LTO phase suggest that CO has been mostly released during taxi-in and taxi-out phases. During taxi procedures, where engines' operation is in idle mode, the volumetric flow rate of air decreases so the fuel combustion is carried out under a lower AFR regime. Consequently, the combustion conditions favor the surplus of carbon contained in fuel which, in turn, increases the presence of CO in the exhaust gases. On the other hand, during the remaining LTO phases, the engines' power settings are greater, the air intake increases, and the CO emissions are more limited (Lieuwen and Yang 2013).

The NO<sub>x</sub> emissions have been noticeably increased during approach/landing, take-off, and climb out compared to those during taxi-in and taxi-out. Increased power settings during take-off and above-the-ground phases provide the engines with significantly greater amounts of air, so increased AFRs sustain a high surplus of nitrogen (N<sub>2</sub>) in the combustion chambers which is contained in the air by approximately 79% (Lieuwen and Yang 2013).

Given that air contains approximately 79% of N<sub>2</sub>, the chemical reaction of fuel combustion ensures a high presence of N<sub>2</sub> in the combustion products. High temperatures inside the engines' combustion chambers favor the transformation of N<sub>2</sub> into NO<sub>x</sub> which they are released to the ambient environment with the exhaust gases. Emissions of PM<sub>2.5</sub>, SO<sub>2</sub>, and CO<sub>2</sub> follow the respective fuel consumption of every LTO phase. The calculated results are provided in [Supplement](#).

The emissions at the Daskalogiannis airport have been much lower than the calculated emissions of large airports such as the Atatürk International Airport (AIA) in Turkey (Kuzu 2018). The annual fuel consumption for the year 2015 in AIA was 277,492 t and the released CO and NO<sub>x</sub> emissions was 2135 t and 4249 t respectively (Kuzu 2018). Fuel consumption at the Daskalogiannis airport during 2016 was 3.29% of the fuel consumption in AIA whereas the produced emissions of CO and NO<sub>x</sub> were 3.08% and 3.20% of the respective emissions in AIA.

In another case study about the Amerigo Vespucci Airport in Florence (Italy), 25,588 flights were performed during 2011 and produced emissions 50.75 t of CO, 59.03 t of NO<sub>2</sub>, and 5.39 t of SO<sub>2</sub> (Simonetti et al. 2015). The airport is of similar capacity in terms of both aircraft traffic, and its emissions are similar to the Daskalogiannis airport.

In addition, aircraft emissions from the Marco Polo Airport in Venice Italy have been studied by Pecorari et al. (2016). Dividing the annual emissions of CO and NO<sub>2</sub> released from Chania airport during 2016 to the number of the year days, it was calculated that the daily emissions of CO and NO<sub>2</sub> were approximately 180 kg and 371 kg, respectively. In comparison, the Marco Polo airport daily emissions of CO and NO<sub>x</sub> during a study in 2009 were estimated to be approximately 1270 kg and 1002 kg, respectively (Pecorari et al. 2016).

## Emission dispersion modeling

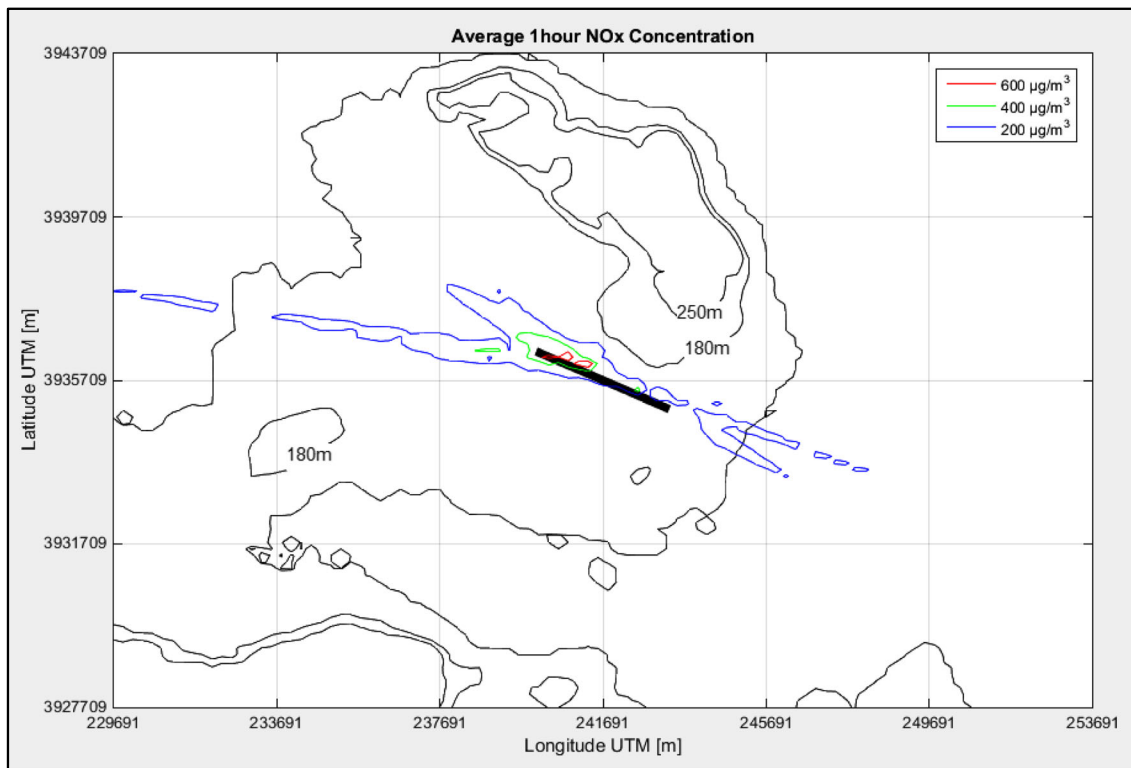
Dispersion modeling has been carried out with EPA's AERMOD model, and the results have been compared to the regulated values described in the European Union Directive 2008/50/EC (EU 2008) to determine the influence of the airport to the local air quality. Aircrafts' emission release has been considered exclusively upward and without the effect of the horizontal momentum of the exhaust gases (Barrett et al. 2013). All the pollutants have been modeled according to the averaging periods mentioned in Directive 2008/50/EC. In addition, modeling of CO<sub>2</sub> has been examined on an annual averaging period in order to be evaluated for its contribution to climate change. The regulated values by 2008/50/EC are provided in [Supplement](#).

The pollutant concentrations at ground level were calculated using the AERMOD model in conjunction with the emission estimations for the LTO cycle. Concerning CO, it was calculated that there has been an accumulation at the northwest of the airport creating a zone of 200 µg/m<sup>3</sup> (8-h average) around the aircraft parking area and the end of runway with a highest value of 345.5 µg/m<sup>3</sup>. These values are quite low in comparison to the maximum regulated 8-h average value of 10,000 µg/m<sup>3</sup> (see [Supplement](#)). Concentrations seem to comply with the wind profile of the area as the concentration contours have an elongated form in parallel with the airport direction. The mountainous shelf of approximate elevation of 200 m at the northeast of the airport suppresses the emissions near to the main runway, whereas the dispersion at the northwest of the airport is more unaffected by this natural obstacle.

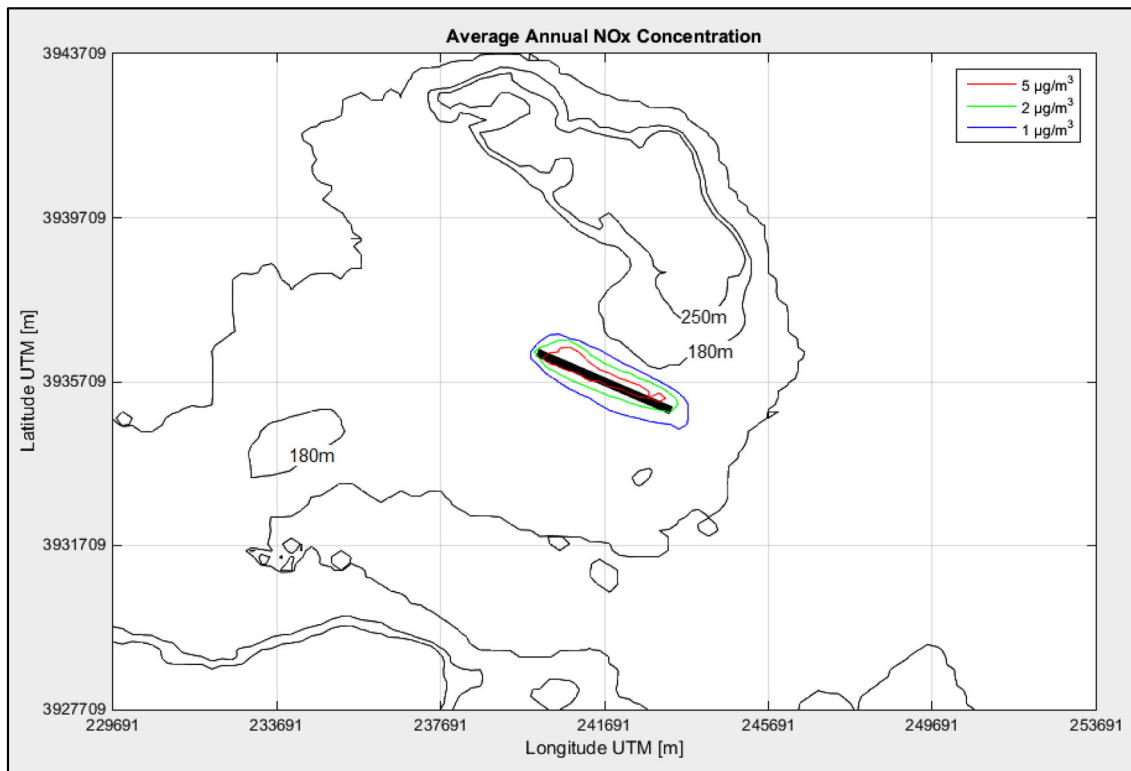
The modeled CO concentrations were quite close to the concentrations measured at a regional airport located in the west side of Romania (Ionel et al. 2011), which has similar traffic capacity to Chania airport. The measurements at this airport refer to a 3 day's period of June 2009, and these were conducted with three different devices at the aircraft's parking area. The results ranged between 250 µg/m<sup>3</sup> and 700 µg/m<sup>3</sup>. The airport traffic for an 8-h period was 35 aircrafts, while the daily average traffic of Chania airport during 2016 was 28 aircrafts. Furthermore, CO emissions from Chania airport during 2016 reached 3.08% of the respective emissions of Atatürk International airport during 2015. The highest modeled value there was 19,839 µg/m<sup>3</sup> (Kuzu 2018) which reflects well its traffic capacity.

The ground-level concentrations of NO<sub>2</sub> have been studied for the averaging period of 1 h and for annual basis as shown in Fig. 3. The model referring to the 1-h average has revealed that there were 20 exceedances of NO<sub>2</sub> concentrations above the value of 200 µg/m<sup>3</sup>; two more than the regulated threshold described in the Directive 2008/50/EC. The exceedances were calculated mostly during the summer period which coincides with the touristic period.

Inside the airport area, especially at the aircraft parking area and the northwest end of runway, NO<sub>2</sub> concentrations have



(a)



(b)

**Fig. 3** Contour plots of NO<sub>2</sub> dispersion concentration calculations at the surface level of **a** average 1 h **b** annual concentration for the year 2016 at Chania airport

been more elevated during the exceedances. In fact, concentrations have reached a value of  $400 \mu\text{g}/\text{m}^3$ , i.e., two times the maximum regulated threshold value. Higher values of three times the threshold value have also been present forming the respective zones. Inside these areas, a maximum value of  $887 \mu\text{g}/\text{m}^3$  has been calculated. The mountainous area has restricted also the dispersion from developing to the northeast of the airport.

Annual dispersion calculations revealed that the concentrations have been lower compared to the regulated value of  $40 \mu\text{g}/\text{m}^3$ . The annual average concentration was more concentrated near to the airport. A zone of  $5 \mu\text{g}/\text{m}^3$  spreads around the main runway and decays spatially to a zone of  $2 \mu\text{g}/\text{m}^3$  and a zone of  $1 \mu\text{g}/\text{m}^3$  as the distance from the airport increases. Inside the zone of  $5 \mu\text{g}/\text{m}^3$ , the maximum calculated value has been  $18 \mu\text{g}/\text{m}^3$ . The topographical anomaly at the northeast of the airport has not influenced the plume morphology to a significant extent.

The maximum annual concentration of  $18 \mu\text{g}/\text{m}^3$  calculated in Chania airport during 2016 has been 3.2% of the annual maximum value calculated in Atatürk International Airport during 2015, since the maximum modeled value at this airport has been  $566 \mu\text{g}/\text{m}^3$  (Kuzu 2018), proving that the relationship between the maximum concentrations at the two airports depends on the ratio of the respective total annual emissions.

Annual  $\text{NO}_x$  emissions of 59 t resulted in concentration values near to the regulated value of  $40 \mu\text{g}/\text{m}^3$  at the parking area of Amerigo Vespucci Airport in 2011 (Simonetti et al. 2015). The maximum concentration of  $\text{NO}_x$  ( $18 \mu\text{g}/\text{m}^3$ ) in Chania airport has been also calculated at the parking area. However, the total emissions during 2016 were about two times greater than those in Amerigo Vespucci Airport during 2011. This discrepancy could be explained by the different aircraft fleet, the different meteorological conditions, and the different area terrain characteristics.

Although 24-h average concentration of  $\text{NO}_x$  is not required to be monitored by any official regulatory context such as the Directive 2008/50/EC, the AERMOD model has been used for the determination of the 24-h average  $\text{NO}_x$  concentration in order to make comparisons with other studies. A study over Marco Polo airport has shown that during two randomly selected days of the year 2009, the daily emissions of  $\text{NO}_x$  have been estimated to be approximately 1002 kg (Pecorari et al. 2016), and the observed  $\text{NO}_x$  concentrations ranged from 10 to  $120 \mu\text{g}/\text{m}^3$  at different sites of the airport.

The calculated daily average of  $\text{NO}_x$  emissions in Chania airport has been calculated equal to 371 kg, which is close to 37% of the emissions of the Marco Polo airport. The maximum concentration value according to the AERMOD calculations was  $70 \mu\text{g}/\text{m}^3$  at the northwest end of the main runway, and there was a zone of  $50 \mu\text{g}/\text{m}^3$  around this peak value. Therefore, the concentration profile of Chania airport was close to 41% of the concentration measured at the Marco

Polo Airport, which corresponds well to the ratio of the total emissions of  $\text{NO}_x$  in the two airports.

The model simulations for 1-h average  $\text{NO}_x$  concentrations showed that there were exceedances from the regulated value of  $200 \mu\text{g}/\text{m}^3$ . A further study was performed with randomly choosing two specific days (20th of January and 20th of July), one during winter and the other during summer. The selection of these 2 days was performed with an aim to study the effect of traffic intensity at the airport. During summer, the traffic intensity is much higher due to charter flights.

According to the traffic data of July 20, 123 LTOs were carried out during this particular day. On the other hand, traffic data of January 20 included only 16 LTOs, which means that the summer traffic was approximately 10 times greater than the winter one. The aircraft fleet composition recorded during these 2 days simply follows the pattern of the annual fleet composition. In particular, Boeing 737-800s performed 6 out of 16 LTOs during the winter day and 47 LTOs during the summer day. An equal share of the summer day traffic was introduced by 767-300s with 47 LTOs, too. Airbus A320s performed 43 LTOs during the summer day.

The summer day simulation revealed that the  $\text{NO}_x$  concentration exceeded approximately three times the regulated value of  $200 \mu\text{g}/\text{m}^3$ . The maximum value of  $546 \mu\text{g}/\text{m}^3$  has been calculated over the main runway. The elevated  $\text{NO}_x$  concentration values were also encountered over the airport and the neighboring sites on the east. Calm conditions have been limited to 16.7% of the day measurements.

Contrary, the winter simulation showed a maximum 1-h concentration equal to  $45 \mu\text{g}/\text{m}^3$  at the northwest of the airport. In these simulations, the emissions are characterized by a limited dispersion concentrated mostly around the main runway and close to the airport. The wind regime mainly consisted of light winds and calm conditions (29.2%) has prevented the emissions from influencing the airport surroundings.

Simulations were also performed for determining the influence of air traffic to the 24-h (see Fig. 4) and annual  $\text{PM}_{2.5}$  mass concentration in the area under study. The model results showed that the contribution is small and the maximum 24-h contribution was  $0.8 \mu\text{g}/\text{m}^3$ . The  $\text{PM}_{2.5}$  dispersion was mainly towards west and northwest direction. Actually, the dispersion has been split to two separate formations in which they have been expanded independently towards these directions. The elevated terrain at the northeast of the airport has played its role as a natural obstacle which has kept the pollutant from dispersing to the north direction. Concerning the annual  $\text{PM}_{2.5}$  concentration, the simulations showed a maximum value of  $0.32 \mu\text{g}/\text{m}^3$  in the aircraft parking area. The calculated values were significantly lower than the regulated maximum value of  $20 \mu\text{g}/\text{m}^3$  (Directive 2008/50/EC). Therefore, airport emissions do not constitute a significant source of  $\text{PM}_{2.5}$  mass in the area under study. Measurements at the Akrotiri research



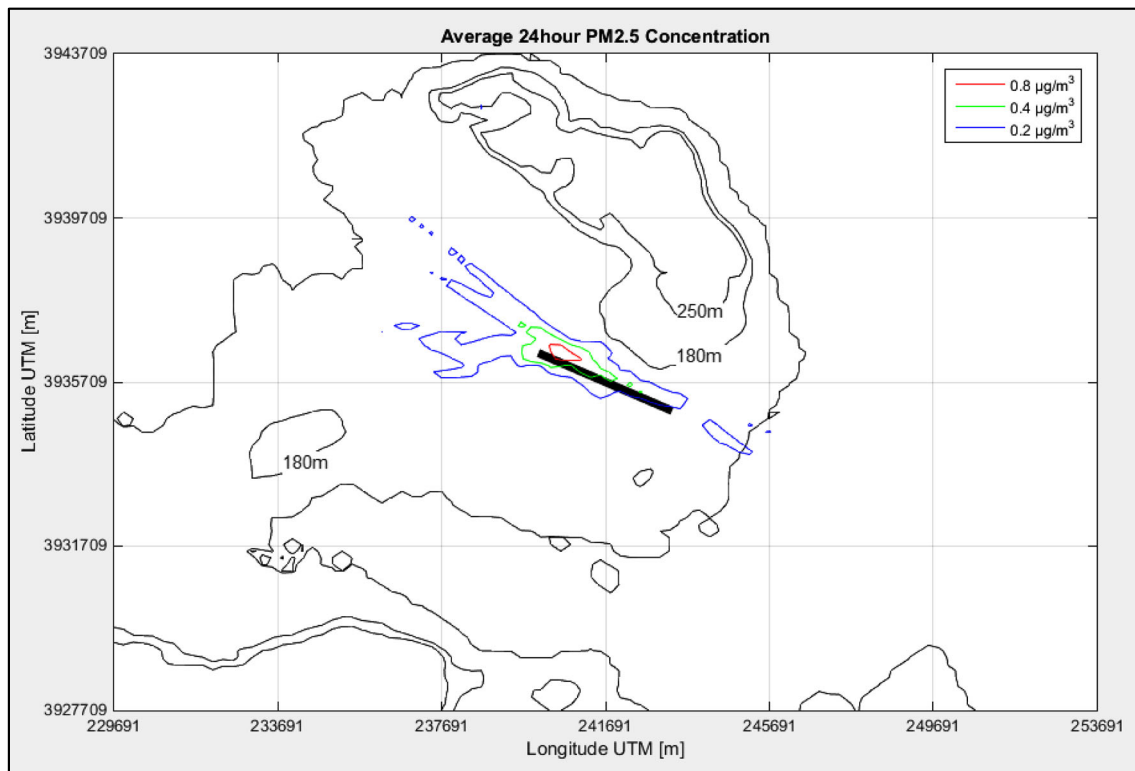


**Fig. 4** Contour plots of 24-h average  $PM_{2.5}$  mass concentration calculations at the surface level for the year 2016 at Chania airport

station which is located 10 km west of the airport showed a mean value of  $PM_{2.5}$  mass equal to  $25.4 \mu\text{g}/\text{m}^3$  during the period 2004–2006 (Lazaridis et al. 2008).

A study over Los Angeles Airport concluded that the daily mean concentration levels of  $PM_{2.5}$  measured during five continuous 24-h intervals in 2005 were between  $32$  and  $42 \mu\text{g}/\text{m}^3$  (Zhu et al. 2011). Another study over the same airport revealed that  $PM_{2.5}$  concentration levels were approximately  $33 \mu\text{g}/\text{m}^3$  in a sampling period, which included six randomly selected weekdays of May and July of 2016 (Shirmohammadi et al. 2017). In the first case, 11 flights were recorded and monitored during 40 min, which implies that the daily activity of this airport was approximately 380 flights.

Even though aircraft engine emissions are not a significant source of particle mass, it constitutes an important source of particle number (Kinsey et al. 2010). The respective particle number emission rates have been calculated according to the methodology described in the “Materials and methods” section.

The yearly average number concentration had a zone of 50,000 particles per  $\text{cm}^3$  at the parking area and values at the airport close to 10,000 particles per  $\text{cm}^3$ . The particles have been transported to the boundaries of the modeling domain with a zone of 1000 particles per  $\text{cm}^3$  close to the boundaries. As for the average 24-h model (see Fig. 5), a zone of 200,000 particles per  $\text{cm}^3$  has been created at the parking area. Moreover, a zone of 100,000 particles per  $\text{cm}^3$  has been

expanded around the main runway. The particulate matter has been transported mostly to the West of the airport creating zones of number concentrations close to 50,000 particles per  $\text{cm}^3$ . However, these values are only indicative since the real concentrations of ultrafine particles were much lower due to coagulation process among ultrafine particles which was not incorporated in the AERMOD. High concentrations of ultrafine particles up to  $10^7$  particles/ $\text{cm}^3$  during aircraft takeoffs were observed from Zhu et al. (2011) at the Los Angeles International airport.

A recent study that was carried out at the international airport of the Greek island of Mytilene in 2014 concluded that the occurrence of ultrafine particles was strongly correlated to the aircraft flight activity, since the mean number concentration of the studied period reached 800,000 particles per  $\text{cm}^3$  (Psanis et al. 2017).

Simulations using the AERMOD were also performed in respect to  $\text{SO}_2$  concentrations (see Supplement). In general, the concentrations of  $\text{SO}_2$  are related both with the fuel consumption profile and the sulfur content in consumed fuel. The model results concluded that the surface  $\text{SO}_2$  concentrations arising from aircraft LTO cycles have been significantly lower than the regulated values described in the Directive 2008/50/EC. For the 1-h average, the maximum concentration value has been  $79 \mu\text{g}/\text{m}^3$  at the location of the parking area at the northwest of the airport which is approximately 22% of the maximum regulated value, i.e.,  $350 \mu\text{g}/\text{m}^3$ . A concentration

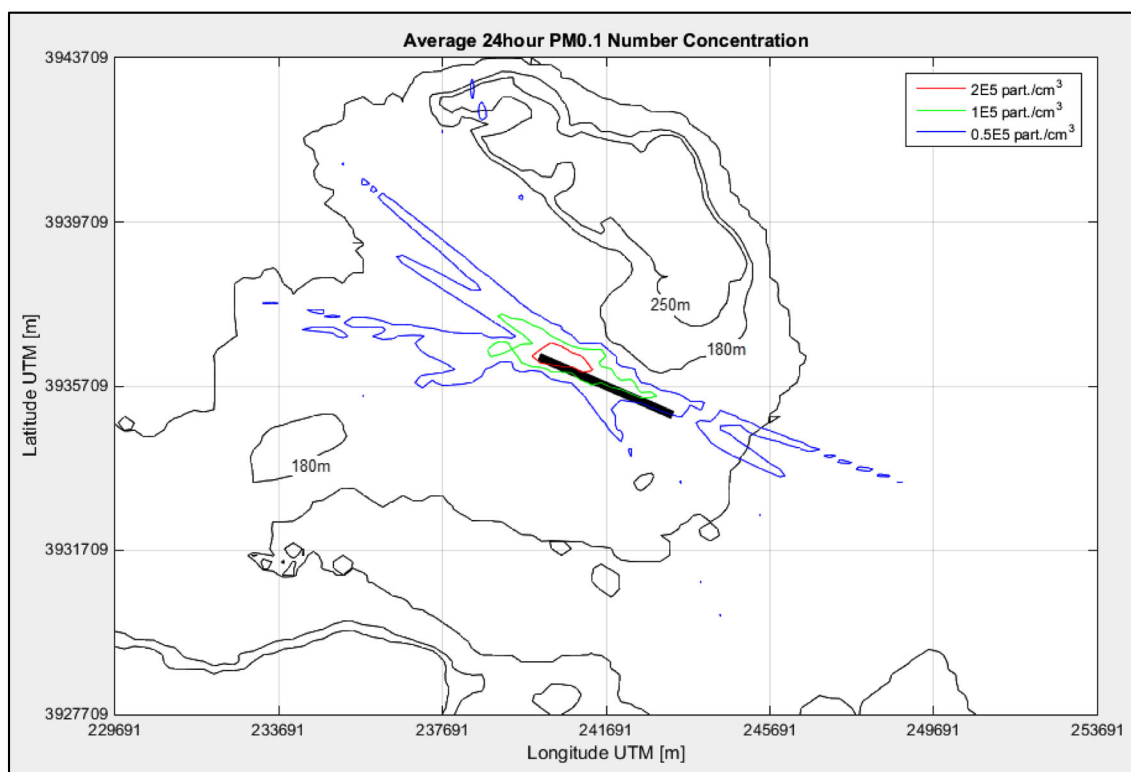


**Fig. 5** Contour plots of 24-h average number concentration of ultrafine particles at the surface level for the year 2016 at Chania airport

zone of  $50 \mu\text{g}/\text{m}^3$  has been formed close to parking area which is followed by a spatial decay of the pollutant concentrations to lower values of  $25 \mu\text{g}/\text{m}^3$ . The dispersion has noticeably affected the northwest areas of the airport whereas the southeast areas have remained unaffected. The average 1-h concentrations have been comparable with the ones produced from an International Romanian Airport with similar traffic characteristics. The  $\text{SO}_2$  concentrations from this airport have not exceeded the level of  $180 \mu\text{g}/\text{m}^3$  (3-min interval) while the most common values ranged between  $35$  and  $85 \mu\text{g}/\text{m}^3$  (Ionel et al. 2011). Concerning the average 24-h simulations, the maximum concentration of  $6.7 \mu\text{g}/\text{m}^3$  has been calculated at the northwest of the airport, also. This value corresponds to the 5.3% of the maximum regulated value which is defined by the Directive 2008/50/EC.

Finally, emissions of  $\text{CO}_2$  were also modeled due to their impact to climate. The total yearly emissions of the airport during 2016 were calculated to be equal to 28,870 t which correspond to the 0.043% of the country's  $\text{CO}_2$  emissions during 2016.

## Conclusions

Emissions and dispersion of air pollutants from LTO cycle of aircrafts at the Chania airport were simulated using the AERMOD model for the year 2016. Hourly meteorological

data were used in the simulations performed and a digital elevation model (DEM) file was applied, which has been obtained from the US Geological Survey (USGS 2018) to derive the surface map of the area of interest. The pollutant emissions were calculated according to the ICAO (2011) methodology, and daily traffic data were used in the simulations.

The dispersion of pollutants was affected from the meteorological conditions and the terrain characteristics. The mountainous formation at the northeast of the airport favors the suppression of the emissions near to the airport runway. Computer simulations revealed that the contribution from aircraft emissions during LTO cycles to the ground-level concentration of  $\text{CO}$ ,  $\text{SO}_2$ , and  $\text{PM}_{2.5}$  mass was not significant. Contrary, the 1-h  $\text{NO}_2$  concentrations exceeded the air quality limits in the area close to the airport due to aircraft engine emissions. The exceedances were performed during the summer period when the air traffic was increased. In addition, ground level of particle number concentrations was calculated to be elevated due to LTO cycles.

The emissions were mainly originated from the ground level part of the LTO cycle. The release height for the above-the-ground operations has been set to 1500 ft., which is the mean height of the LTO cycle, and the influence to the ground-level concentration of pollutants was negligible.

The above results demonstrate the importance of the aircraft traffic emissions, especially  $\text{NO}_2$  and fine particles, to human exposure, both inside the airport affecting personnel

and travelers and near the airport affecting local communities. Consequently, specific measures have to be taken for reducing the air traffic mainly during the summer period.

**Funding information** The present work was supported by the project “PANhellenic infrastructure for Atmospheric Composition and climate change” (MIS 5021516) which is implemented under the Action “Reinforcement of the Research and Innovation Infrastructure” funded by the Operational Programme “Competitiveness, Entrepreneurship and Innovation” (NSRF 2014–2020), and co-financed by Greece and the European Union (European Regional Development Fund).

## References

- Barrett SRH, Britter RE, Waitz IA (2013) Impact of aircraft plume dynamics on airport local air quality. *Atmos Environ* 74:247–258
- Campell P, Zhang Y, Yan F, Lu ZF, Streets D (2018) Impacts of transportation sector emissions on future US air quality in a changing climate. Part I: projected emissions, simulation design and model evaluation. *Environ Pollut* 238:903–917
- Carlsaw DC, Beevers SD, Ropkins K, Bell MC (2006) Detecting and quantifying aircraft and other on-airport contributions to ambient nitrogen oxides in the vicinity of a large international airport. *Atmos Environ* 40:5424–5434
- EMEP (2017) EMEP/EEA air pollutant emission inventory guidebook 2016
- EU (2008) Directive 2008/50/EC of the European Parliament and of the Council of 21 May 2008 on Ambient Air Quality and Cleaner Air for Europe
- Flightradar 24 (2018) <http://www.flightradar24.com>. Accessed 10 Jan 2018
- ICAO (2008) Environmental Protection: Annex, 16, Vol. II, Aircraft Engine Emissions
- ICAO (2011) Document 9889. Airport Air Quality Manual ISBN 978–92–9231–862–8
- ICAO (2018) Engine Emissions Data Bank. <https://www.easa.europa.eu/easa-and-you/environment/icao-aircraft-engine-emissions-databank>. Accessed 4 Apr 2018
- Intergovernmental Panel on Climate Change (IPCC) (1999) Aviation and the global atmosphere. Summary for Policymakers
- Intergovernmental Panel on Climate Change (IPCC) (2006) Guidelines for National Greenhouse Gas Inventories
- Ionel D, Nicolae F, Popescu C, Talianu LB, Apostol G (2011) Measuring air pollutants in an international Romania airport with point and open path instruments. *Rom J Phys* 56:507–519
- Kinsey JS, Dong Y, Williams DC, Logan R (2010) Physical characterization of the fine particle emissions from commercial aircraft engines during the aircraft particle emissions eXperiment (APEX) 1–3. *Atmos Environ* 44:2147–2156
- Kuzu SL (2018) Estimation and dispersion modeling of landing and take-off (LTO) cycle emissions from Atatürk International Airport. *Air Qual Atmos Health* 11:153–161
- Lazaridis M, Dzumbova L, Kopanakis I, Ondracek J, Glytsoy T, Aleksandropoulou V, Voulgarakis A, Katsivela E, Mihalopoulos N, Eleftheriadis K (2008) PM<sub>10</sub> and PM<sub>2.5</sub> levels in the eastern Mediterranean. *Water Air Soil Pollut* 189(1–4):85–101
- Lieuwen TC, Yang V (2013) Gas turbine emissions. Cambridge University Press
- Masiol M, Harrison RM (2014) Aircraft engine exhaust emissions and other airport-related contributions to ambient air pollution: a review. *Atmos Environ* 95:409–455
- Mazaheri M, Johnson GR, Morawska L (2009) Particle and gaseous emissions from commercial aircraft at each stage of the landing and takeoff cycle. *Environ Sci Technol* 43:441–446
- Ogimet. <https://www.ogimet.com/metars.phtml.en>. Accessed 4 Nov 2017
- Pecorari E, Mantovani A, Franceschini G, Bassanoc D, Palmeri L, Rampazzo G (2016) Analysis of the effects of meteorology on aircraft exhaust dispersion and deposition using a Lagrangian particle model. *Sci Total Environ* 541:839–856
- Petzold CS, Nyeki S, Gysel M, Weingartner E, Baltensperger U, Giebl H, Hitznerberger R, Doppelheuer A, Vrchoticky S, Pyxbaum H, Johnson M, Hurley CD, Marsh R, Wilson CW (2003) Properties of jet engine combustion particles during the PartEmis experiment: microphysics and chemistry. *Geophys Res Lett* 30(13):1719
- Psanis C, Triantafyllou E, Giamarelou M, Manousakas M, Eleftheriadis K, Biskos G (2017) Particulate matter pollution from aviation-related activity at a small airport of the Aegean Sea Insular Region. *Sci Total Environ* 596:187–193
- Shirmohammadi F, Sowlat MH, Hasheminassab S, Saffari A, Ban-Weiss G, Sioutas C (2017) Emission rates of particle number, mass and black carbon by the Los Angeles International Airport (LAX) and its impact on air quality in Los Angeles. *Atmos Environ* 151:82–93
- Simonetti I, Maltagliati S, Manfrida G (2015) Air quality impact of a middle size airport within an urban context through EDMS simulation. *Transp Res D* 40:144–154
- Testa E, Giammusso C, Bruno M, Magiore P (2013) Fluid dynamic analysis of pollutants’ dispersion behind an aircraft engine during idling. *Air Qual Atmos Health* 6:367–383
- USEPA (2016) User’s guide for the AMS/EPA regulatory model (AERMOD). EPA-454/B-16-011, December, 2016
- USGS (2018) US Geological Survey <https://earthexplorer.usgs.gov/>. Accessed 15 Mar 2018
- Yang X, Cheng S, Lang J, Xu R, Lv Z (2018) Characterization of aircraft emissions and air quality impacts of an international airport. *J Environ Sci* 72:198–207
- Yilmaz I (2017) Emissions from passenger aircraft at Kayseri airport, Turkey. *J Air Transp Manag* 58:176–182
- Yin F, Grewe V, Frömming C, Yamashita H (2018) the formation of persistent contrails for transatlantic flights. *Transp Res D* 65:466–484
- Zhu Y, Fanning E, Yu RC, Zhang Q, Froines JR (2011) Aircraft emissions and local air quality impacts from takeoff activities at a large International Airport. *Atmos Environ* 45:6526–6533

**Publisher’s note** Springer Nature remains neutral with regard to jurisdictional claims in published maps and institutional affiliations.